Palaeogeography, Palaeoclimatology, Palaeoecology 620 (2023) 111574

Contents lists available at ScienceDirect

Palaeogeography, Palaeoclimatology, Palaeoecology

journal homepage: www.elsevier.com/locate/palaeo

Using the factors of soil formation to assess stable carbon isotope disequilibrium in late Pleistocene (MIS 3) buried soils of the Great Plains, North America

Anthony L. Layzell *, Greg A. Ludvigson, Jon J. Smith, Rolfe D. Mandel

Kansas Geological Survey, 1930 Constant Ave., Lawrence, KS 66047, USA

ARTICLE INFO

Editor: Dr A Dickson

Keywords:
Paleosols
Loess
Gilman Canyon Formation
Pedogenic carbonate
Soil organic matter

ABSTRACT

The stable carbon isotope composition of both soil organic matter (SOM) and pedogenic carbonate are widely used as paleoenvironmental proxies. This study utilizes $\delta^{13}C$ analyses to reconstruct bioclimatic change from a series of buried soils in the central Great Plains of North America that developed between ca. 44–24 ka. Results revealed a paradoxical isotopic disequilibrium between the isotopic composition of bulk SOM ($\delta^{13}C_{SOM}$) and pedogenic carbonate ($\delta^{13}C_{carb}$). Specifically, $\mathbf{\Delta}^{13}C$ values are 0.1 to 6.3 per mil greater than the highest expected equilibrium value of 17 per mil in the Bk horizons. In contrast, $\mathbf{\Delta}^{13}C$ values are 0.1 to 4.8 per mil lower than the lowest expected equilibrium value of 14 per mil in the Ak horizons. A soil-forming factor approach was utilized to establish multiple working hypotheses regarding the influence of climate, vegetation, parent material, and time on the observed isotopic disequilibrium.

Of the various hypotheses presented, we suggest that the following most likely explain the observed isotopic disequilibrium. The greater-than-expected $\mathbf{\Delta}^{13}C$ values in the Bk horizons most likely reflects seasonal bias in pedogenic carbonate formation, resulting in an apparent C_4-biased signal. The lower-than-expected $\mathbf{\Delta}^{13}C$ values in the Ak horizons remains perplexing. The most likely explanation is that detrital carbonate contributions affected the $\delta^{13}C_{carb}$ record or that the $\delta^{13}C_{carb}$ and $\delta^{13}C_{SOM}$ records are asynchronous. Overall, it appears that different factors have affected the $\delta^{13}C_{SOM}$ and $\delta^{13}C_{carb}$ records independently and therefore results of this study highlight the importance of assessing pedogenic carbonates for isotopic equilibrium as well as the need to understand past environmental conditions (i.e., soil-forming factors) when interpreting isotopic trends.

1. Introduction

The five factors of soil formation (climate, organisms, relief, parent material, and time; clorpt) are one of the most widely known frameworks for understanding soil genesis (Jenny, 1941; Birkeland, 1999; Amundson, 2021). Where factors function as independent variables, individual factors can be investigated by holding the other factors constant. This approach has been successfully used to study climosequences (e.g., Webb et al., 1986; Chadwick et al., 2003; Driese et al., 2005), toposequences (e.g., Yair, 1990; Beach et al., 2018; Deressa et al., 2018), parent material sequences (Treadwell-Steitz and McFadden, 2000), chronosequences (e.g., Tonkin and Basher, 2001; Dorji et al., 2009; Layzell et al., 2012) as well as the relationships between the different factors (e.g., Birkeland et al., 2003; Stiles et al., 2003; Eppes et al., 2008; Johnson et al., 2015; Turner et al., 2018). The soil forming factor approach is particularly helpful when studying paleosols (e.g., buried soils) as paleosols serve as important archives of paleoenvironmental information and landscape history.

A variety of properties from buried soils have been investigated to provide insights on landscape evolution and paleoenvironmental change, including soil morphology, clay content, carbonate accumulation, elemental composition, mineralogy, and magnetic susceptibility (e.g., Alekseeva et al., 2007; Jacobs and Mason, 2007; Eppes et al., 2008; Beach et al., 2018). In the Great Plains of North America, the stable carbon isotope compositions of soil organic matter (SOM) in buried soils have especially proven useful for reconstructing late Quaternary bioclimatic change (e.g., Fredlund and Tieszen, 1997; Johnson and Willey, 2000; Nordt et al., 2008; Mandel, 2008; Layzell and Mandel, 2020). Regional studies utilizing the isotopic composition of Quaternary pedogenic carbonates in buried soils, however, are far more scarce (e.g.,

* Corresponding author.
E-mail address: alayzell@ku.edu (A.L. Layzell).

https://doi.org/10.1016/j.palaeo.2023.111574
Received 30 November 2022; Received in revised form 8 March 2023; Accepted 17 April 2023
Available online 20 April 2023

Kelly et al., 1991; Humphrey and Ferring, 1994; Tecsa et al., 2020). Here, we investigate a series of buried soils from the central Great Plains that date to Marine Isotope Stage (MIS) 3. Paleoenvironmental change in this region during MIS 3 remains unclear due to the lack of well-dated high-resolution proxy records (Dorale et al., 1998; Voelker, 2002). Therefore, isotopic analyses were performed on both bulk SOM and pedogenic carbonates to reconstruct late Quaternary plant communities and infer paleoclimatic change in the region. In turn, we demonstrate how the factors of soil formation can be used as a framework to assess the reliability of stable carbon isotopes as paleoenvironmental proxies.

1.1. Geology and loess stratigraphy

The study area (Fig. 1) is located in western Kansas and is part of the High Plains section of the Great Plains physiographic province. The High Plains is characterized by predominantly flat terrain with relief (5–20 m) being largely confined to river valleys, dune fields and numerous small playa basins. The region represents the remnant of a vast alluvial plain formed by sediment shed eastward from the Rocky Mountains. These deposits mostly comprise the Miocene and early Pliocene-aged Ogallala Formation together with Quaternary alluvial and eolian sediments. Loess deposits blanket the High Plains surface, ranging in thickness from >20 m in parts of Nebraska to <5 m in southwestern Kansas (Bettis et al., 2003). At least four Quaternary-aged loess units have been documented in the region: the Loveland Loess, Gilman Canyon Formation (GCF), Peoria Loess and Bignell Loess (e.g., Bettis et al., 2003; Layzell et al., 2016).

The GCF overlies the Loveland-Sangamon complex and is usually <2 m thick on the Great Plains (Bettis et al., 2003), and consists of a dark silt loam that has been modified by episodes of cumulic soil development (e.g., Reed and Dreeszen, 1965; Mandel and Bettis, 1995; Johnson et al., 2007). Published ages (calibrated radiocarbon and optically stimulated luminescence) from sites in the central Great Plains range from ca. 44–24 ka (Johnson et al., 2007; Muhs et al., 2008; Layzell et al., 2016).

The Peoria Loess mantles the GCF and is the thickest, most extensive loess deposit in the Great Plains (Bettis et al., 2003). The Peoria Loess typically is a light yellowish tan to brown silt loam. Peoria Loess accumulated in the Great Plains between ca. 25–13 ka (Bettis et al., 2003; Mason et al., 2007; Muhs et al., 2008). After ca. 13 ka, the Brady Geosol developed in the Peoria Loess but is only distinguishable from the modern surface soil when buried by the Bignell Loess. The Brady Soil typically is a dark gray to grayish brown silt loam with a well-expressed B horizon (Johnson and Willey, 2000). The Bignell Loess began to accumulate between ca. 11–9 ka, but deposition was spatially and temporally variable throughout the Holocene (Mason et al., 2003; Muhs et al., 2008; Tecsa et al., 2020).

1.2. Stable carbon isotopes

$\delta^{13}C$ values determined on SOM ($\delta^{13}C_{SOM}$) from buried soils reflect the relative contributions of C_3 and C_4 vegetation to below ground biomass production at the time of soil formation. Modern C_3 plant communities include trees, woody shrubs, and cool season grasses and typically have $\delta^{13}C_{SOM}$ values between −32‰ and − 20‰ with a mean of −27‰ (Kohn, 2010). In contrast, C_4 plants, which include warm season grasses, have $\delta^{13}C_{SOM}$ values between −14‰ and − 10‰, with a mean of −13‰.

$\delta^{13}C$ values from pedogenic carbonate ($\delta^{13}C_{carb}$) also can be used to assess past vegetation compositions. Pedogenic carbonate forms in carbon isotopic equilibrium with soil CO_2, which is derived mainly from root respiration and therefore reflects the relative contributions of C_3 and C_4 species. $\delta^{13}C_{carb}$ values are offset, however, by 14–17‰ relative to $\delta^{13}C_{SOM}$ due to molecular diffusion of soil-respired CO_2 and isotopic equilibria reactions between CO_2 and calcite (Cerling et al., 1989).

2. Methods

2.1. Coring

Three cores were collected in the study area to examine regional loess stratigraphy. Two continuous 6.5 cm diameter cores (HP1A and CMC) were collected from the High Plains surface in southwestern

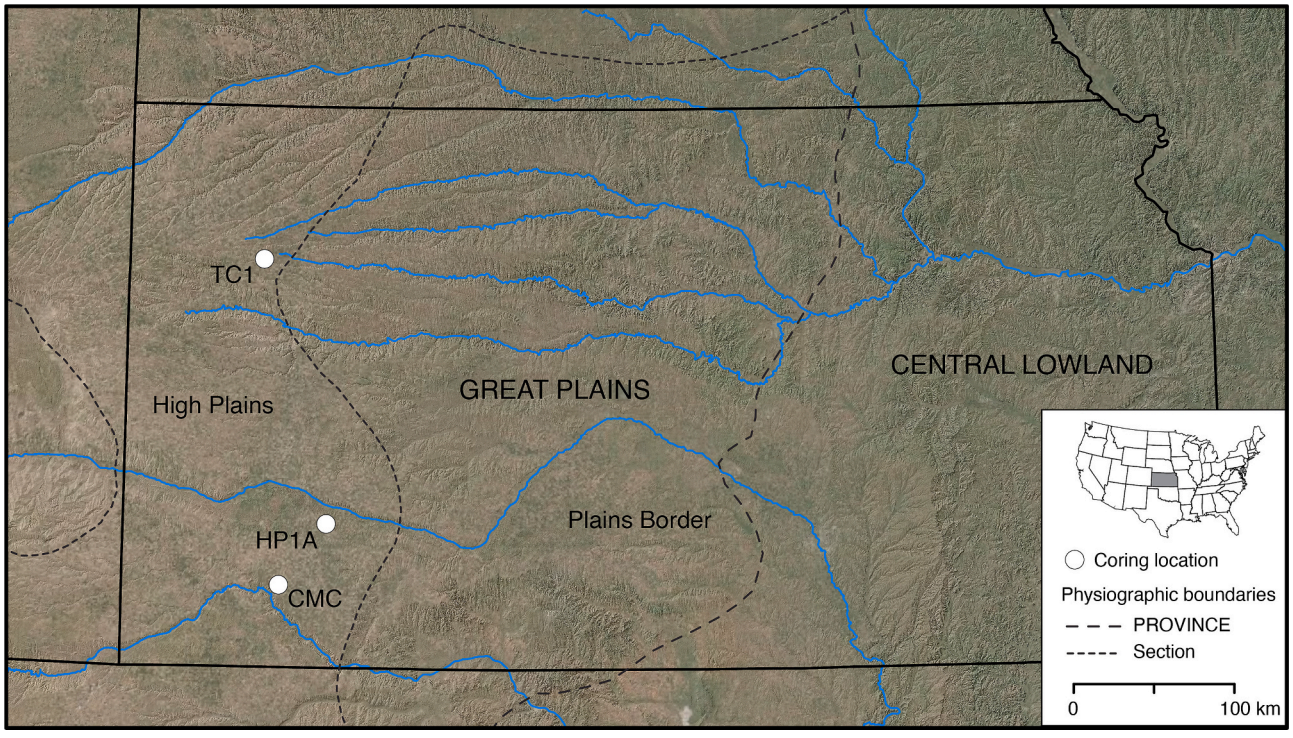

Fig. 1. Map showing locations of cores HP1A (37°39′25″, 100°39′53″), CMC (37°26′47″, 101°03′43), and TC1 (39°13′11″, 101°00′54) in the High Plains Section of the Great Plains Physiographic Province.

Kansas and one core (TC1) from northwestern Kansas (Fig. 1) as part of the High Plains Ogallala Drilling Program at the Kansas Geological Survey. Drilling and core retrieval were accomplished using an Acker hollow-stem auger and wireline, split-spoon core sampler.

2.2. Soil properties

Soils were described and sampled using standard terminology (see Birkeland, 1999; Schoeneberger et al., 2012) and sampled by horizon for particle size analysis. However, where horizon thicknesses were > 50 cm, subsamples were collected and analyzed. Particle-size distribution was determined using the pipette method (Gee and Bauder, 1986). Percent calcium carbonate equivalent (CCE) and organic carbon were determined during stable carbon isotope sample preparation and analysis, respectively (see section 2.3).

2.3. Stable carbon isotopes

Stable carbon isotope analyses were performed on bulk SOM ($\delta^{13}C_{SOM}$) and pedogenic carbonates ($\delta^{13}C_{carb}$) to investigate past vegetation compositions in the region. All stable isotopic analyses were performed at the University of Kansas W.M. Keck Paleoenvironmental and Environmental Stable Isotope Laboratory following methods outlined by Boutton (1996). Bulk SOM samples were collected at regular intervals (15–30 cm) from core. Samples were dried, ground with a mortar and pestle, and approximately 1 g of ground sample was extracted for decarbonation. Decarbonation consisted of adding 30 ml of 0.5 M HCl to each sample and agitating on a vortex mixer after 1 h and approximately every 4 h thereafter over a 24-h period. This decarbonation procedure was repeated until samples no longer visibly reacted to additional HCl. Samples were then repeatedly rinsed by adding 30 ml of DI water, centrifuging at 4000 rpm for 6 min, and then decanting rinse water until supernatant reached a neutral pH. Rinsed samples were oven dried at 50 °C and re-homogenized with a synthetic ruby mortar and pestle. Weighing samples before and after desiccation allowed for the determination of percent calcium carbonate equivalent (CCE). Decarbonated samples were combusted using a Costech Elemental Analyzer at 1060 °C and the resultant CO_2 analyzed by a continuous-flow ThermoFinnigan MAT 253 mass spectrometer. The Elemental Analyzer also reports the percentage of carbon in the sample. All $\delta^{13}C$ data were calibrated with in-house and international standards (DORM, USGS 24, IAEA C6, IAEA 600) and are presented relative to the Vienna Peedee Belemnite (VPDB) standard. Analytical precision is better than 0.10‰. A simple mass balance equation was used to estimate the relative contribution of C_4 plants to SOM:

$$\delta^{13}C_{SOM} = \delta^{13}C_{C4}(x) + \delta^{13}C_{C3}(x)\ (1-x)$$

where $\delta^{13}C_{SOM}$ is the measured $\delta^{13}C$ value, $\delta^{13}C_{C4} = -13‰$, $\delta^{13}C_{C3} = -27‰$ and x is the relative contribution (%) of C_4 plants to SOM.

The isotopic composition of pedogenic carbonate ($\delta^{13}C_{carb}$) was determined from discrete nodules (2–8 mm diameter) that were collected from the same intervals as SOM samples where present in the A and B horizons of the soils. Individual nodules were powdered and analyzed with a Kiel III device coupled to a dual inlet ThermoFinnigan MAT 253 mass spectrometer. Analytical precision is monitored by daily analysis of NBS-19 and NBS-18 and is better than 0.10‰.

The isotopic composition of organic matter occluded within carbonate nodules ($\delta^{13}C_{OOM}$) was also analyzed and compared to $\delta^{13}C_{SOM}$ values. Organic matter was extracted from select nodules following procedures designed to remove carbonate minerals and concentrate any finely disseminated occluded organic matter within the acid-treated residue. Individual nodules were initially reacted with 30 ml of 0.5 M HCl until they no longer effervesced, then reacted with 1 ml of 12 M HCl solution for at least 24 h. Fresh aliquots of HCl were added every 12 h until no further reaction could be detected. Samples were then rinsed and analyzed as outlined above for bulk SOM samples.

In this paper we use the ‰ symbol for measured $\delta^{13}C$ values relative to VPDB and the term “per mil” to refer to the magnitude of difference between measured $\delta^{13}C$ values. The $\Delta^{13}C$ notation is used to indicate the difference between $\delta^{13}C$ values determined on SOM and pedogenic carbonate ($\delta^{13}C_{carb\ -\ SOM}$).

2.4. Micromorphology

Samples of core containing pedogenic carbonate nodules from buried soil horizons in the CMC and HP1A cores were vacuum impregnated with epoxy resin, thin sectioned, and micropolished. Thin sections (0.03 mm) were investigated with a Reliotron III cathodoluminescence (CL) imaging system at the Kansas Geological Survey to assess diagenetic alteration. Microscopic images were collected under transmitted light and CL using an Olympus DP73 17 mpx digital camera mounted on an Olympus BX41 microscope.

2.5. Chronology

Numerical-age control was provided by radiocarbon (^{14}C) dating of SOM. In addition, we utilize two ^{14}C ages and two optically stimulated luminescence (OSL) ages obtained from the HP1A and CMC cores, reported in Layzell et al. (2016). Radiocarbon samples from the TC1 core were submitted to DirectAMS Inc. for processing, including standard physical and chemical pretreatment to remove roots and carbonates. All radiocarbon dates were calibrated (Table 1), and in the text of this paper are presented as median calibrated ages.

Table 1
Age information.

Radiocarbon ages

Core	Lab no.	Depth (m)	^{14}C age (yr B.P.)	Calibrated age range[2] (yr B.P.)	Median calibrated age (ka)
CMC	D-AMS021617	2.0	19,900 ± 75	24,150–23,780	23.9
CMC[1]	OS-112461	2.8	24,900 ± 840	30,870–27,590	29.1
CMC[1]	OS-112462	3.2	30,300 ± 1700	38,775–31,130	34.7
TC1	D-AMS037071	8.1	22,600 ± 95	27,210–26,460	27.0
TC1	D-AMS037072	8.7	27,430 ± 145	31,680–31,160	31.4
TC1	D-AMS037073	9.1	29,030 ± 110	33,960–33,180	33.6
TC1	D-AMS023229	9.4	31,490 ± 150	36,200–35,450	35.9

OSL ages

Core	Lab no.	Depth (m)	No. of aliquots	Dose Rate (Gy/ka)	De ± 2σ (Gy)	OD (%)	OSL age ± 2σ (ka)
HP1A[1]	USU-1110	3.9	29 (46)	3.39 ± 0.16	150.08 ± 21.79	37.2 ± 5.4	44.3 ± 7.8
CMC[1]	USU-1518	4.4	8 (55)	2.79 ± 0.14	145.36 ± 22.24	17.2 ± 6.5	52.2 ± 9.6

[1] Data originally reported in Layzell et al. (2016).
[2] Calibration (2 sigma) was performed with CALIB 8.1 using calibration dataset IntCal20.

3. Results

3.1. Soils and stratigraphy

All three cores contain surface and buried soils developed in late-Quaternary eolian parent materials (Fig. 2). In the HP1A and CMC cores, the upper stratum is about 2 m thick and comprises the Peoria Loess. The upper stratum in the TC1 core is about 75 cm thick and is interpreted as comprising the Bignell Loess. The surface soil (Soil 1) is similar in all three cores and has a moderately expressed A-Bk-Ck profile. Horizon thicknesses of the surface soil, however, are less in the TC1 core. Soil 2 in the TC1 core has a moderately expressed Ak-Bk-Ck profile and is interpreted as the Brady Soil developed in Peoria Loess. The thickness of the Peoria Loess in the TC1 core is substantially greater (~7 m) than the other two cores, likely reflecting a more proximal location to loess sources. Also, the Peoria Loess in the HP1A and CMC cores has a relatively high clay content (Fig. 3), suggesting a location more distal to loess sources.

All three cores contain a buried soil (Soil 2 in cores HP1A and CMC; Soil 3 in core TC1), interpreted as representing a soil developed in the GCF (Fig. 2). Soil morphology is similar in all three cores, consisting of a moderate to well-expressed Ak-Bk-Ck profile. The Ak horizons range in thickness from 1 to 1.25 m and consist of very dark grayish brown to brown (10YR 3/2 to 4/3) silty clay loams with subangular to angular blocky structure. The blocky structure of the Ak horizons is likely a product of the relatively high clay contents (21–36%) (Fig. 3). Common fine threads and films of calcium carbonate and few fine (< 5 mm) spheroidal carbonate nodules occur in the Ak horizons (Stage I-II). Calcium carbonate equivalent values range from 2.2 to 11.7% (Fig. 3). The Bk horizons are between 60 and 80 cm thick and have yellowish brown colors (10YR 5/4 to 6/4) and loam, silty clay loam, and clay loam textures with subangular to angular blocky structure. Calcium carbonate equivalent values range from 12.4 to 24.8% (Fig. 3). Secondary carbonate accumulations consist of common fine (< 1 cm) spheroidal nodules, threads, and films (Stage II). The texture of the Ck horizons in the HP1A and CMC cores consists of sandy loam compared to silt loam and clay loam in the TC1 core (Fig. 3). The upward-fining sequence evident in Soil 2 from the HP1A and CMC cores has been interpreted as reflecting an increase in loess deposition relative to more locally derived eolian sands during soil formation (Layzell et al., 2016).

OSL samples from the Ck horizons of Soil 2 in the HP1A and CMC cores yielded ages of 44.3 and 52.2 ka, respectively (Layzell et al., 2016). SOM from the upper and lower 10 cm of the Akb1 horizon and the upper 10 cm of the Bkb1 horizon of Soil 2 in the CMC core yielded ages of 24.0, 29.2 and 34.6 ka, respectively (Table 1). A suite of three ^{14}C samples from the Akb2 horizon and one sample from the upper 10 cm of the Bkb2 horizon of Soil 3 in the TC1 core yielded ages of 26.9, 31.3, 33.3 and 35.4 ka, respectively. In sum, the numerical chronology indicates that soil development began shortly after ca. 44 ka and continued for approximately 20 ky. The deposition of Peoria Loess buried the GCF soil between ca. 27–24 ka, though burial occurred earlier at the TC1 core locality, likely reflecting a location closer to loess sources. Regional studies have provided remarkably similar ages of ca. 45–24 ka for the GCF (e.g., Souders and Kuzila, 1990; Johnson et al., 2007; Muhs et al., 2008) as well as for coeval buried soils developed in alluvial fills (e.g., Layzell et al., 2015; Mandel et al., 2016).

3.2. Stable carbon isotopes

In the HP1A core, $\delta^{13}C_{SOM}$ values from the GCF soil (Soil 2) increase from an average of −23.5‰ in the Ckb horizons to −15.6‰ at the top of the Akb horizon (Fig. 2). This latter value indicates the presence of a C_4-

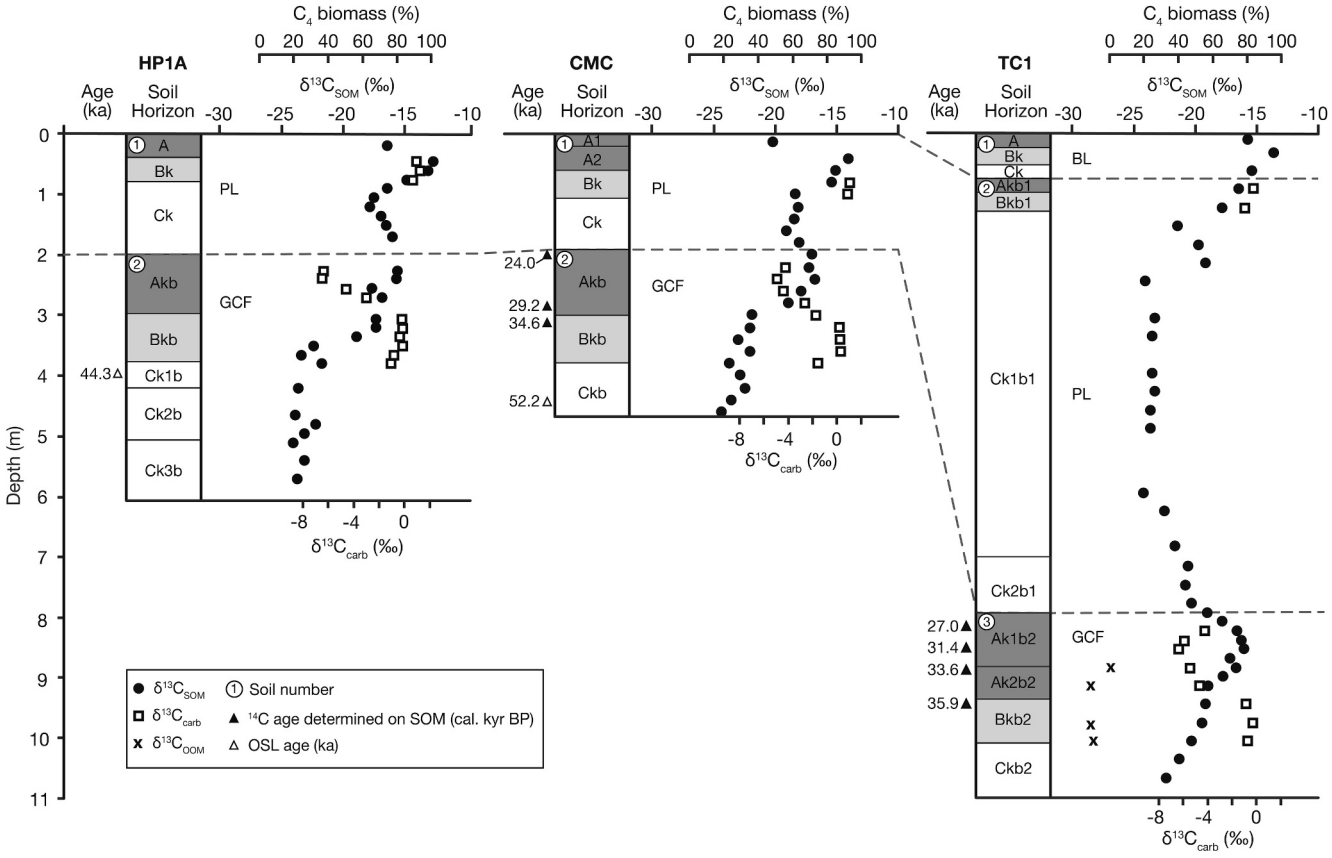

Fig. 2. Soil stratigraphy, chronology, and stable carbon isotope profiles from cores HP1A, CMC, and TC1. BL = Bignell Loess, PL = Peoria Loess, GCF = Gilman Canyon Formation. Note that the $\delta^{13}C_{carb}$ axis is positioned to reflect a 15 per mil offset relative to $\delta^{13}C_{SOM}$.

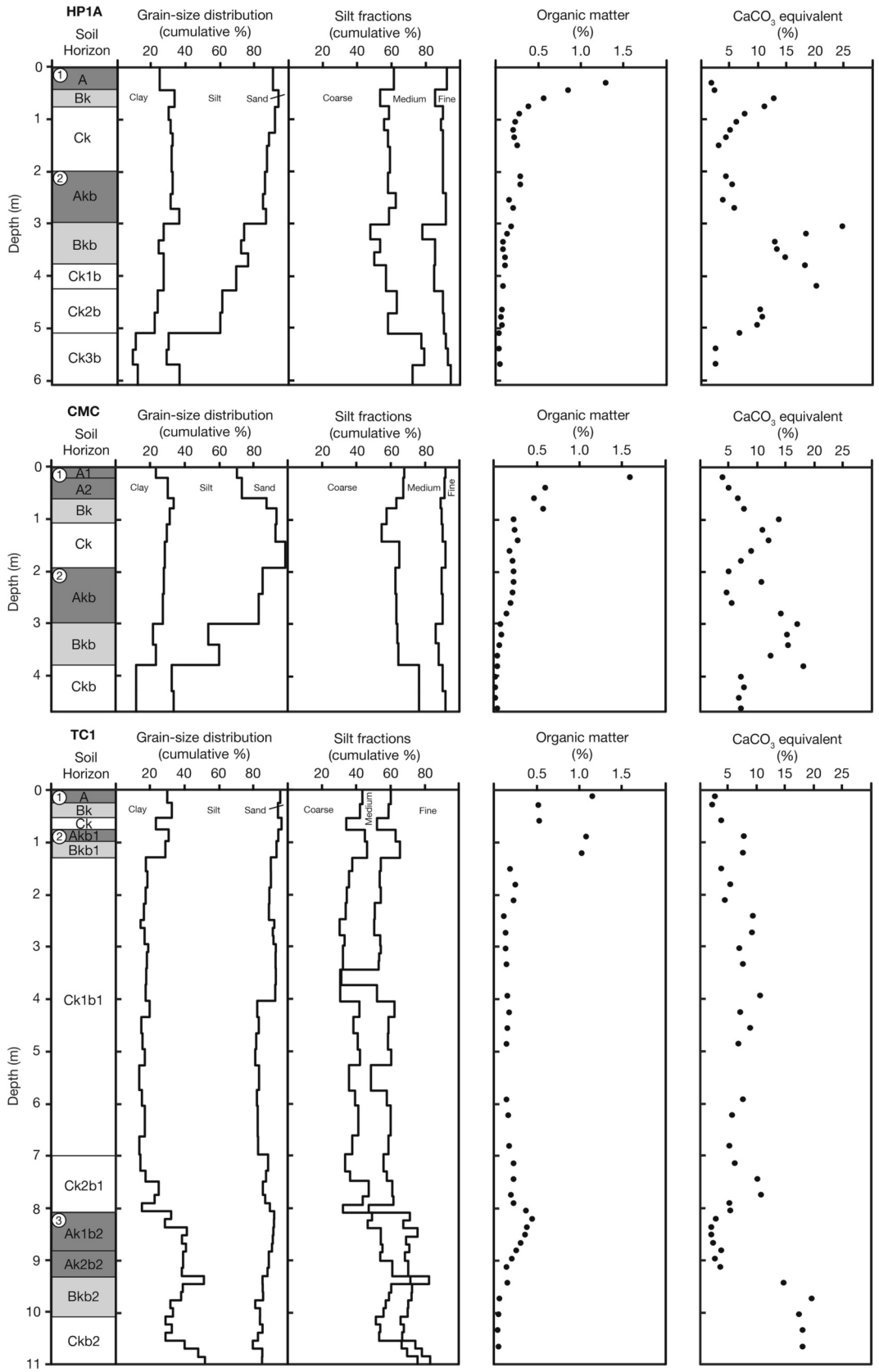

Fig. 3. Particle size, organic carbon and calcium carbonate equivalent data from the three cores. Particle size fractions: sand (2000–50 μm); silt (50–2 μm), coarse silt (50–20 μm); medium silt (20–5 μm), fine silt (5–2 μm); clay (< 2 μm). Particle size data for HP1A and CMC cores is from Layzell et al. (2016).

dominated plant community with C_4 biomass contributing up to 81% of organic carbon to the soil. $\delta^{13}C_{SOM}$ values are relatively high in the Ck horizon of Soil 1 (average of −17.1‰), likely reflecting detrital contributions of organic matter, and increase to a peak of −12.7‰ (100% C_4 biomass) near the top of the modern surface soil.

Trends in $\delta^{13}C_{SOM}$ values from the CMC core are similar to those in the HP1A core. $\delta^{13}C_{SOM}$ values from the GCF soil (Soil 2) increase from an average of −23.3‰ in the Ckb horizon to −17.0‰ (71% C_4 biomass) at the top of the Akb horizon (Fig. 2). $\delta^{13}C_{SOM}$ values become slightly more negative in the Ck horizon of Soil 1 (average of −18.4‰) before increasing to peak at −14.1‰ (92% C_4 biomass) near the top of the modern surface soil.

In core TC1, $\delta^{13}C_{SOM}$ values from the GCF soil (Soil 3) increase from −22.3‰ at the bottom of the soil to −16.5‰ at the top (Fig. 2). The peak $\delta^{13}C_{SOM}$ value of −15.9‰ occurs at a depth of 8.5 m and indicates the presence of up to 79% C_4 biomass. $\delta^{13}C_{SOM}$ values become more negative in the Ckb1 horizons of Soil 2 (average of −20.0‰) before increasing to −16.4‰ at the top of Soil 2 (the Brady Soil), reflecting an increase in the amount of C_4 biomass (up to 76%). The surface soil (Soil 1) has the highest $\delta^{13}C_{SOM}$ value of −13.5‰ (up to 96% C_4 biomass).

$\delta^{13}C_{SOM}$ values show consistent depth trends in the soils, becoming less negative upward through the solum (Fig. 2). $\delta^{13}C_{carb}$ values, however, appear to have the opposite trend, decreasing upward through the soil profile. $\delta^{13}C_{carb}$ values from the Bk horizons of the GCF soil are similar in all three soils. In the HP1A core, Bk horizon $\delta^{13}C_{carb}$ values are relatively invariant and range from −0.1‰ to −1.0‰. In the CMC core, $\delta^{13}C_{carb}$ values are uniform in the middle part of the Bkb horizon, ranging between 0.2‰ and 0.3‰, with more negative values of −1.8‰ and − 1.6‰ at the top and bottom of the horizon, respectively. In the TC1 core, Bkb2 horizon $\delta^{13}C_{carb}$ values range from −0.3‰ to −0.9‰. The $\delta^{13}C_{carb}$ values in the Bk horizons of the GCF soils are similar to those recorded in the Bk horizon of the Brady Soil (−0.2‰ to −0.9‰) but slightly more negative than those from the Bk horizons of the surface soils (0.7‰ to 1.3‰).

At the bottom of the Ak horizons of the GCF soils, $\delta^{13}C_{carb}$ values shift and start to become more negative relative to values in the Bk horizons. $\delta^{13}C_{carb}$ values peak in the middle to upper part of the Ak horizons and are significantly more negative compared to the Bk horizons (Fig. 2). In the HP1A core, $\delta^{13}C_{carb}$ values in the Akb horizon range from −3.0‰ to −6.5‰. In the CMC core, $\delta^{13}C_{carb}$ values for the Akb horizon range between −2.7‰ and − 4.9‰, whereas in the TC1 core, $\delta^{13}C_{carb}$ values for the Ak1b2 and Ak2b2 horizons range from −4.3‰ to −6.4‰.

The $\delta^{13}C$ results indicate an apparent lack of carbon isotopic equilibrium between $\delta^{13}C_{carb}$ and $\delta^{13}C_{SOM}$ in the GCF soils. $\mathbf{\Delta}^{13}C$ values ($\delta^{13}C_{carb - SOM}$) in the Bk horizons are 0.1 to 6.3 per mil greater than the highest expected equilibrium value of 17 per mil (see Cerling et al., 1989) (Fig. 4). In contrast, $\mathbf{\Delta}^{13}C$ values in the Ak horizons are 0.1 to 4.8 per mil lower than the lowest expected equilibrium value of 14 per mil.

4. Discussion

Using a soil-forming factor approach allows for the establishment of multiple working hypotheses regarding the influence of climate, vegetation, parent material, and time on the observed trends in $\delta^{13}C$ values and, specifically, the documented carbon isotopic disequilibrium between $\delta^{13}C_{carb}$ and $\delta^{13}C_{SOM}$. In the following discussion, we consider the effect of changes in temperature, aridity, seasonality, water saturation, and carbon sources during MIS 3 as well as potential changes in parent material contributions and diagenetic overprinting over time.

4.1. Stable carbon isotopic composition of soil organic matter

$\delta^{13}C_{SOM}$ values increase upward through the GCF soil profiles, indicating an increase in the contribution of C_4 biomass during soil formation. Specifically, $\delta^{13}C_{SOM}$ results from the Bk horizons of three soils developed in the GCF, indicate a transition from a C_3-dominated plant community with up to 26% C_4 biomass to a C_4-dominated plant community with up to 69% C_4 biomass between ca. 44–35 ka. $\delta^{13}C_{SOM}$

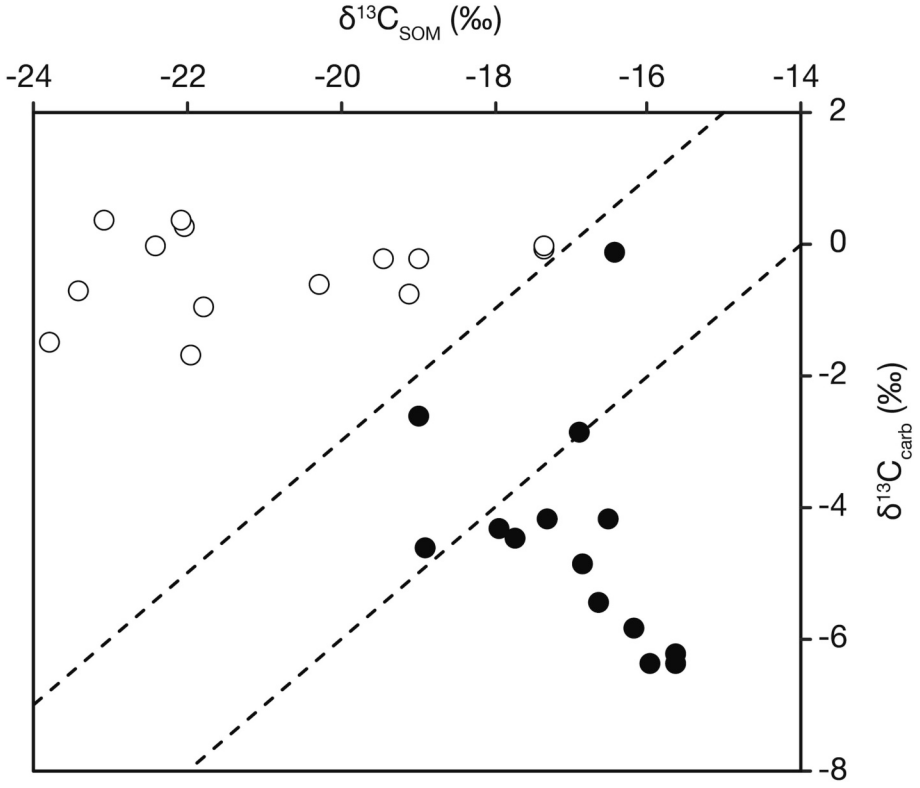

Fig. 4. Plot of $\delta^{13}C_{SOM}$ vs $\delta^{13}C_{carb}$ for samples from the GCF soils. Filled symbols = Ak horizons; Open symbols = Bk horizons. Area between dashed lines indicates theoretical offset of 14–17 per mil between $\delta^{13}C_{SOM}$ and $\delta^{13}C_{carb}$ values (see Cerling et al., 1989).

results from the Ak horizons of the GCF soils, indicate the presence of a C_4-dominated ecosystem with C_4 biomass contributing between 57% and 81% of organic carbon to the soil from ca. 35–24 ka. The regional dominance of C_4 vegetation during late MIS 3 was likely favored by lower atmospheric CO_2 levels before the Last Glacial Maximum (e.g., Ehleringer et al., 1997). However, other environmental factors favoring C_4 plants, including summer temperature, aridity, and the seasonal distribution of rainfall (e.g., Terri and Stowe, 1976; von Fischer et al., 2008; Knapp et al., 2020), likely played a role.

It is important to note that the more negative $\delta^{13}C_{SOM}$ values in the Bk horizons may reflect a greater contribution of detrital organic material to the isotopic signal as pedogenic inputs of organic carbon are lower in subsurface horizons. For example, percent carbon in the GCF soils ranges from 0.05% to 0.17% in the Bk horizons compared to between 0.15% and 0.45% in the Ak horizons (Fig. 3). The higher proportion of organic carbon in the Ak horizons makes it more likely that any detrital isotopic signal will be overridden. However, the carbon content in the GCF soils is still relatively low compared to the surface soils and the Brady soil, which have >1% organic carbon. SOM in buried soils is susceptible to decomposition, which can result in ^{13}C enrichment of several per mil relative to the original biomass (Wynn, 2007). Furthermore, the degree of ^{13}C enrichment increases with lower organic carbon content. Given the low carbon content in the GCF soils, we cannot rule out the effect of ^{13}C enrichment from decomposition on the reported $\delta^{13}C_{SOM}$ values. However, in the TC1 core, for example, the peak organic carbon content in the GCF Ak horizon is about 40% that of the surface and Brady soils, suggesting that any enrichment from decomposition is likely on the order of 1–2 per mil (see Wynn, 2007). Such an effect does not alter our observation that plant communities during late MIS 3 were dominated by C_4 grasses based on the $\delta^{13}C_{SOM}$ record.

4.2. Comparison between stable carbon isotopic composition of soil organic matter and pedogenic carbonate

The $\delta^{13}C$ results indicate an apparent lack of carbon isotopic equilibrium between $\delta^{13}C_{carb}$ and $\delta^{13}C_{SOM}$ in the GCF soils. Specifically, $\mathbf{\Delta}^{13}C$ values in the Bk horizons are greater than expected equilibrium values whereas $\mathbf{\Delta}^{13}C$ values in the Ak horizons are lower than expected. Given these findings, several hypotheses regarding the effect of climate, vegetation, parent material, and time on the formation of pedogenic carbonate must be considered.

4.2.1. Climate and vegetation

The diffusion gradient of CO_2 in a soil is well documented and reflects two-component CO_2 mixing with changing contributions of atmospheric CO_2 and soil-respired CO_2 with depth (e.g., Cerling, 1984; Quade et al., 1989). Generally, mixing of atmospheric CO_2 is minimal at soil depths of 30–50 cm and a majority of carbonate nodules sampled were collected at depths of >30 cm from the interpreted paleosurface. Changes in temperature, aridity, and associated soil productivity, however, can affect the isotopic record of pedogenic carbonate by altering the diffusion gradient of CO_2 in a soil. For example, more arid conditions with associated low plant density and reduced respiration rates allows for a greater degree of atmospheric CO_2 mixing in the soil (e.g., Pendall et al., 1994; Montañez, 2013). Similarly, lower winter temperatures allow for increased additions of atmospheric CO_2 into the soil through freezing and frost heave (e.g., Cerling, 1984; Stevenson et al., 2005). Because atmospheric CO_2 is more enriched in ^{13}C than soil CO_2, increased depth of atmospheric CO_2 penetration could explain the higher-than-expected $\mathbf{\Delta}^{13}C$ values in the Bk horizons of the GCF soils but not, however, the lower-than-expected values in the Ak horizons.

Another hypothesis is that the positive enrichment of up to 6 per mil in $\delta^{13}C_{carb}$ for Bk horizons reflects seasonal bias in pedogenic carbonate formation. Breecker et al. (2009) suggest that pedogenic carbonates only form during the summer in semi-arid environments when the soil is dry and moisture stress strongly limits respiration rates. Therefore, $\delta^{13}C_{carb}$ values are biased toward a C_4 signal and may be enriched in semi-arid soils by 2–3 per mil. This may explain the greater-than-expected $\mathbf{\Delta}^{13}C$ values in the Bk horizons. However, for samples where ^{13}C enrichment is >3 per mil, one must also invoke concomitant effects such as that of detrital organic matter on the $\delta^{13}C_{SOM}$ signal. Breecker et al. (2009) also postulate that wet-dry cycles may be required for pedogenic carbonate formation. Therefore, the presence of pedogenic carbonates in the GCF soils indicates that climatic conditions at the time of soil formation must have been seasonally dry, reflecting either monsoonal or frequent drought conditions.

Finally, regarding the less-than-expected $\mathbf{\Delta}^{13}C$ values in the Ak horizons, another hypothesis related to climate is that the pedogenic carbonate in the Ak horizon formed in water-saturated conditions. Studies have shown that phases of carbonate formation, reflecting formation during water-saturated parts of the year, had significantly more negative $\delta^{13}C$ values than carbonate that formed in well-drained conditions (e.g., Mintz et al., 2011; Tabor et al., 2013). This hypothesis can be rejected, however, as there is no morphological evidence of water-saturated conditions (e.g., gleying, mottling, or other redoximorphic features) in the GCF soils.

4.2.2. Parent material

Particle size analyses indicate both a notable increase in the proportion of silt and clay in the Ak horizons of the GCF soils (Fig. 3). These textural observations likely signify increased inputs of loess and fine dust during pedogenesis (e.g., Jacobs and Mason, 2005, 2007; Layzell et al., 2016). Hence, the Ak horizons of the GCF soils are a product of cumulization processes, where soil formation was able to keep pace with sedimentation, resulting in soil upbuilding (e.g., Birkeland, 1999).

Cumulization processes could have affected the isotopic signal of pedogenic carbonates in the Ak horizons in three ways. First, because the paleosurface was aggrading we cannot be confident that carbonate nodules sampled originally formed at depths >30 cm. It is possible that carbonate nodules formed at shallower depths, which would allow for a greater influence of atmospheric CO_2 on the isotopic signal. However, as previously noted (see Section 4.2.1.) atmospheric CO_2 effects would result in higher-than-expected $\mathbf{\Delta}^{13}C$ values rather than the lower-than-expected values documented in the Ak horizons.

Second, additions of detrital carbonate in the form of loess and dust, derived from either carbonate bedrock or older reworked pedogenic carbonate, may have provided a third component to CO_2 through subsequent dissolution processes. Most studies investigating the effect of three-component CO_2 mixing in soils have focused on marine carbonate bedrock parent materials (e.g., Quade et al., 1989; Wang et al., 1996; Monger et al., 1998; Kraimer and Monger, 2009; Michel et al., 2013). Contributions of CO_2 from the dissolution of marine carbonates are typically ^{13}C-enriched relative to the other two components of CO_2 (i.e., soil and atmospheric sources). Therefore, if carbonate bedrock was a significant carbon source, then more positive $\delta^{13}C_{carb}$ values would be expected in contrast to the more negative values recorded in the Ak horizons. Fewer studies have investigated the contributions of fine-grained detrital carbonates from eolian sources; however, most assume that dissolution of fine-grained detrital carbonate will equilibrate with soil CO_2 and thereby not provide a unique carbon source for pedogenic carbonate (e.g., Pendall et al., 1994; Wang et al., 1996; Tabor et al., 2013).

Finally, the isotopic signal of detrital carbonate may have been physically occluded into the pedogenic carbonate. If that is the case then, the observed negative trend in $\delta^{13}C_{carb}$ values upward through the Ak horizon could reflect increasing contributions of detrital carbonate from loess and fine dust deposition that was subsequently occluded by pedogenic carbonate nodules during Ak horizon formation. Mineralogical, geochemical, and isotopic studies have shown that the loess in the central Great Plains is primarily sourced from siltstones of the White River Group with additional contributions from the Arikaree Group and

fine-grained facies of the Ogallala Formation (e.g., Aleinikoff et al., 2008; Muhs et al., 2008). Yang et al. (2017) reported similar results from western Nebraska, though deposition of the basal Peoria Loess and GCF included a greater contribution of material from Rocky Mountain sources. $\delta^{13}C_{carb}$ values for the White River Group have been shown to range between −6‰ and − 7‰ (Mullin, 2010) whereas $\delta^{13}C_{carb}$ values for Ogallala Group carbonates range between −3.5‰ and − 6.5‰ (Gardner et al., 1992). Those values are notably similar to $\delta^{13}C_{carb}$ values in the Ak horizons of the GCF soils. It is therefore feasible that this detrital isotopic signal was incorporated into the pedogenic carbonates of the GCF Ak horizons. CL analyses indicate that detrital carbonate is present in the form of small (<10 μm) grains that exhibit orange luminescence (Fig. 5 B and D). Detrital carbonate grains are predominantly present in the soil matrix with minor amounts occluded within the nodules. Therefore, given the volumetric difference between detrital and authigenic carbonate it is unlikely that isotopic signal of the nodule was altered by detrital material.

4.2.3. Time

The first consideration in terms of the effect of time on the observed isotopic disequilibrium between $\delta^{13}C_{carb}$ and $\delta^{13}C_{SOM}$ is that of post-formational diagenetic alteration of authigenic carbonates. Studies have shown that pedogenic carbonates can undergo diagenetic alteration over time in the presence of dissolved inorganic groundwater carbon (e.g., Deutz et al., 2001; Budd et al., 2002; Michel et al., 2016). To assess the degree of potential diagenetic alteration of pedogenic carbonate nodules, thin sections were examined via petrographic techniques and CL imaging. The visible light CL emittance from different carbonate components provides information on the oxidation state of the soil water at the time of formation and the possible presence of recrystallization.

Pedogenic nodules in both the Ak and Bk horizons exhibit non-luminescence indicating formation in an oxidizing vadose depositional environment (Fig. 5B and D). There is no evidence for orange Mn-activated CL luminescence, indicating that there has not been overprinting in reducing phreatic groundwaters, nor multiple dissolution-precipitation events over time. Moreover, unimodal crystal size domains in the nodules as opposed to juxtapositions of micritic and microspar domains indicates that the nodules retain a primary record. Overall, carbonate nodules in the GCF soils exhibit the ideal petrographic and CL characteristics recommended for conducting paleoenvironmental reconstructions (see Michel et al., 2016).

A second hypothesis related to the time factor is that the $\delta^{13}C_{carb}$ and $\delta^{13}C_{SOM}$ records are asynchronous. Studies have shown that secondary carbonates in the form of nodules and rhizoliths can form post-depositionally (e.g., Gocke et al., 2011) and may therefore be in isotopic equilibrium with a different carbon pool (e.g., Kelly et al., 1991; Wang et al., 1993; Budd et al., 2002). In this case, Ak horizon pedogenic carbonate may have formed in isotopic equilibrium with a later soil carbon pool that was dominated by C_3 biomass. The observed progressive negative shift in $\delta^{13}C_{carb}$ values during Ak horizon formation may be reflective of the progressive development of a C_3-dominated carbon pool (Fig. 3). However, SOM turnover in silt and clay-dominated soils typically occur over tens to hundreds of years (Balesdent et al., 1988) whereas the turnover rate for pedogenic carbonate occurs over thousands of years or longer (e.g., Amundson et al., 1988; Cerling and Quade, 1992; Wang et al., 1993). It is therefore surprising that a later C_3-dominated carbon pool is not reflected in the bulk $\delta^{13}C_{SOM}$ data.

In order to investigate this hypothesis further, we tested whether $\delta^{13}C$ values from bulk SOM and organic matter occluded in carbonate nodules were similar. Occluded organic matter samples from the Ak horizon (8.8 and 9.1 m depth) and the Bk horizon (9.8 and 10.1 m depth) in the TC1 core yielded $\delta^{13}C_{OOM}$ values between −26.8‰ and − 28.4‰ (Fig. 2). Bulk $\delta^{13}C_{SOM}$ values at comparable depths range between −16.6‰ and − 20.2‰, suggesting the presence of a unique occluded organic matter source. However, like the bulk SOM, the occluded organic matter is not in isotopic equilibrium with the pedogenic carbonate. The $\Delta^{13}C$ values between occluded organic matter and pedogenic carbonate range from −21.3 to −28.1 per mil and are therefore 4.3 to 11.1 per mil greater than the highest expected equilibrium value of 17

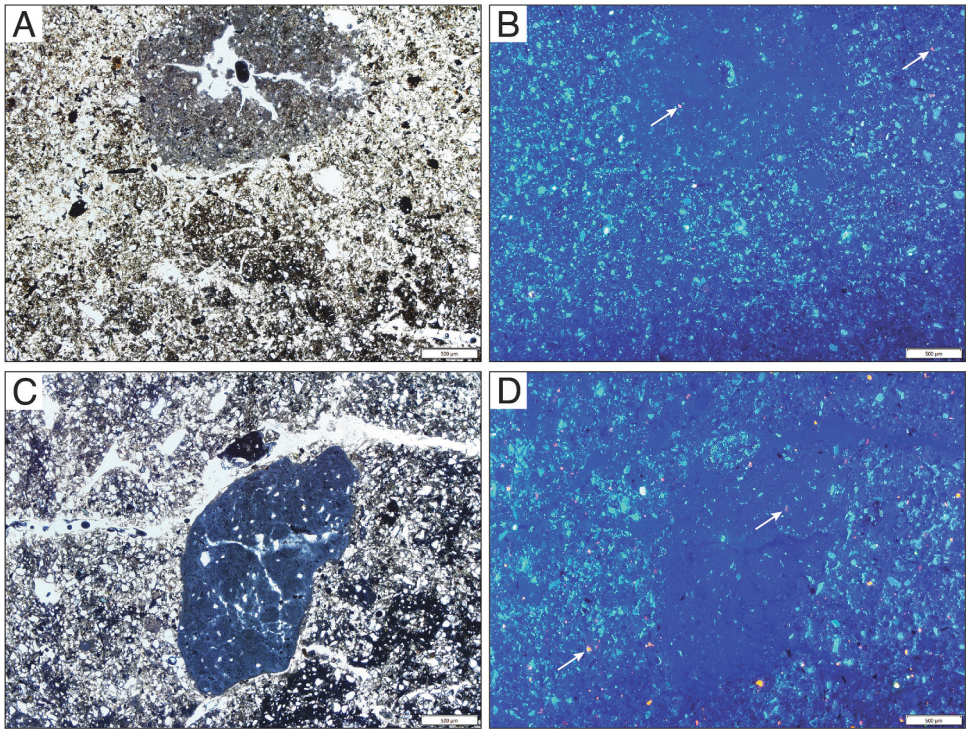

Fig. 5. Microscopic images of carbonate nodules from the TC1 core. (A) and (B) show a nodule from the Akb2 horizon under transmitted light and cathodoluminescence, respectively. (C) and (D) show a nodule from the Bkb2 horizon under transmitted light and cathodoluminescence, respectively. Whites arrows in (B) and (D) point to examples of detrital carbonate grains.

per mil. Hence, the most parsimonious explanation is that the occluded organic matter represents a detrital component that is unrelated to the observed isotopic trends in $\delta^{13}C_{carb}$ values.

An interesting finding is that $\delta^{13}C_{carb}$ values in the Ak horizons of the GCF appear to be in isotopic equilibrium with bulk $\delta^{13}C_{SOM}$ values from the overlying C horizons of the Peoria Loess. For example, in the Ck horizon of Soil 1 in the CMC core $\delta^{13}C_{SOM}$ values range from −19.1‰ to −18.1‰. Comparing these values to the $\delta^{13}C_{carb}$ values of the Ak horizon of Soil 2 results in $\mathbf{\Delta}^{13}C$ values ranging between −16.4‰ and −13.2‰, with most values within the expected offset range of 14–17 per mil. Similarly, in the TC1 core, $\delta^{13}C_{SOM}$ values in the Ck2b1 horizon of the Peoria Loess range from −20.7‰ to −18.9‰. Comparing these values to the $\delta^{13}C_{carb}$ values of the Ak horizon of Soil 3 indicates $\mathbf{\Delta}^{13}C$ values ranging between −16.4 and − 12.5 per mil, with most values within the expected range of 14–17 per mil. Also, the negative shift in bulk $\delta^{13}C_{SOM}$ values in the C horizons of the Peoria Loess is mirrored in the $\delta^{13}C_{carb}$ values but at a greater depth. For example, the $\delta^{13}C_{SOM}$ record indicates a trend of increasing C_3 biomass in the TC1 core between 8.1 and 7.4 m depth whereas the $\delta^{13}C_{carb}$ record indicates a similar shift between 9.4 and 8.5 m depth (Fig. 2).

One possible mechanism for the patterns described above is the penetration of roots from C_3 plants growing during Peoria Loess deposition into the Ak horizon that provided the carbon source (i.e., respired CO_2) for secondary carbonate formation. However, while the drop in pCO_2 may have facilitated carbonate precipitation in the form of rhizoliths and hypocoatings along root traces, it is unclear how root respired CO_2 would facilitate carbonate nodule formation, especially when the isotopic composition of the bulk SOM in the Ak horizon appears to have been unaffected. Also, it should be noted that a potential relationship between Ak horizon $\delta^{13}C_{carb}$ values of the GCF and bulk $\delta^{13}C_{SOM}$ values in the overlying Peoria Loess is not seen in the HP1A core. In sum, while it is possible that the SOM and pedogenic carbonate in the Ak horizons formed asynchronously, without numerical ages on the pedogenic carbonate we can neither confirm nor refute this hypothesis.

5. Conclusions

Given that the stable carbon isotopic composition of both SOM and pedogenic carbonate are widely used as paleoenvironmental proxies, the results of this study have important implications for interpreting and understanding the fidelity of the paleoenvironmental record. Isotopic analyses of SOM and pedogenic carbonate nodules from buried soils that developed between ca. 44–24 ka on the High Plains of western Kansas revealed paradoxical isotopic disequilibrium between $\delta^{13}C_{SOM}$ and $\delta^{13}C_{carb}$. $\mathbf{\Delta}^{13}C$ values are 0.1 to 6.3 per mil greater than the highest expected equilibrium value of 17 per mil in the Bk horizons. In contrast, $\mathbf{\Delta}^{13}C$ values are 0.1 to 4.8 per mil lower than the lowest expected equilibrium value of 14 per mil in the Ak horizons.

A soil-forming factor approach was utilized to establish multiple working hypotheses regarding the influence of climate, vegetation, parent material, and time on the observed trends in $\delta^{13}C$ values. Of the various hypotheses presented, we suggest that the following most likely explain the observed isotopic disequilibrium. The greater-than-expected $\delta^{13}C_{carb}$ values in the Bk horizons most likely reflects seasonal bias in pedogenic carbonate formation, resulting in a C_4-biased signal. The lower-than-expected $\delta^{13}C_{carb}$ values in the Ak horizons remains perplexing. We suggest that the effects of parent material, through detrital carbonate contributions, and time (i.e., that $\delta^{13}C_{carb}$ and $\delta^{13}C_{SOM}$ records are asynchronous) are the most plausible explanations. However, with the available evidence we are unable to definitively explain the observed isotopic disequilibrium in the Ak horizons. Overall, it appears that different factors have affected the $\delta^{13}C_{SOM}$ and $\delta^{13}C_{carb}$ records independently and therefore results of this study highlight the importance of assessing pedogenic carbonates for isotopic equilibrium as well as the need to understand past environmental conditions (i.e., soil-forming factors) when interpreting isotopic trends. In this regard, the utilization of other independent proxies in conjunction with stable isotope records is warranted.

Declaration of Competing Interest

The authors declare that they have no known competing financial interests or personal relationships that could have appeared to influence the work reported in this paper.

Data availability

Data will be made available on request.

Acknowledgments

We extend our gratitude to the various landowners for kindly allowing us access to their property and to Bruce Barnett for processing isotope samples at KPESIL.

Funding: This work was supported by the United States Geological Survey [STATEMAP program], the Geological Society of America [Graduate Student Research Grant], the Society for Sedimentary Geology [SEPM Foundation Award], and the National Science Foundation [NSF EAR-1023285].

Appendix A. Supplementary data

Supplementary data to this article can be found online at https://doi.org/10.1016/j.palaeo.2023.111574.

References

Alekseeva, T., Alekseev, A., Maher, B.A., Demkin, V., 2007. Late Holocene climate reconstructions for the Russian steppe, based on mineralogical and magnetic properties of buried palaeosols. Palaeogeogr. Palaeoclimatol. Palaeoecol. 249 (1–2), 103–127. https://doi.org/10.1016/j.palaeo.2007.01.006.

Aleinikoff, J.N., Muhs, D.R., Bettis III, E.A., Johnson, W.C., Fanning, C.M., Benton, R., 2008. Isotopic evidence for the diversity of late Quaternary loess in Nebraska: glaciogenic and nonglaciogenic sources. Geol. Soc. Am. Bull. 120 (11–12), 1362–1377. https://doi.org/10.1130/B26222.1.

Amundson, R., 2021. Factors of soil formation in the 21st century. Geoderma 391, 114960. https://doi.org/10.1016/j.geoderma.2021.114960.

Amundson, R.G., Chadwick, O.A., Sowers, J.M., Doner, H.E., 1988. Relationship between climate and vegetation and the stable carbon isotope chemistry of soils in the eastern Mojave Desert,Nevada. Quat. Res. 29 (3), 245–254. https://doi.org/10.1016/0033-5894(88)90033-6.

Balesdent, J., Wagner, G.H., Mariotti, A., 1988. Soil organic matter turnover in long-term field experiments as revealed by carbon-13 natural abundance. Soil Sci. Soc. Am. J. 52 (1), 118–124. https://doi.org/10.2136/sssaj1988.03615995005200010021x.

Beach, T., Luzzadder-Beach, S., Cook, D., Krause, S., Doyle, C., Eshleman, S., Wells, G., Dunning, N., Brennan, M.L., Brokaw, N., Cortes-Rincon, M., Hammond, G., Terry, R., Trein, D., Ward, S., 2018. Stability and instability on Maya Lowlands tropical hillslope soils. Geomorphology 305, 185–208. https://doi.org/10.1016/j.geomorph.2017.07.027.

Bettis III, E.A., Muhs, D.R., Roberts, H.M., Wintle, A.G., 2003. Last glacial loess in the conterminous USA. Quat. Sci. Rev. 22 (18–19), 1907–1946. https://doi.org/10.1016/S0277-3791(03)00169-0.

Birkeland, P.W., 1999. Soils and Geomorphology. Oxford University Press, New York.

Birkeland, P.W., Shroba, R.R., Burns, S.F., Price, A.B., Tonkin, P.J., 2003. Integrating soils and geomorphology in mountains—an example from the Front Range of Colorado. Geomorphology 55 (1–4), 329–344. https://doi.org/10.1016/S0169-555X(03)00148-X.

Boutton, T.W., 1996. In: Stable carbon isotope ratios of soil organic matter and their use as indicators of vegetation and climate change. Mass spectrometry of soils, pp. 47–82.

Breecker, D.O., Sharp, Z.D., McFadden, L.D., 2009. Seasonal bias in the formation and stable isotopic composition of pedogenic carbonate in modern soils from Central New Mexico, USA. Geol. Soc. Am. Bull. 121 (3–4), 630–640. https://doi.org/10.1130/B26413.1.

Budd, D.A., Pack, S.M., Fogel, M.L., 2002. The destruction of paleoclimatic isotopic signals in Pleistocene carbonate soil nodules of Western Australia. Palaeogeogr. Palaeoclimatol. Palaeoecol. 188 (3–4), 249–273. https://doi.org/10.1016/S0031-0182(02)00588-6.

Cerling, T.E., 1984. The stable isotopic composition of modern soil carbonate and its relationship to climate. Earth Planet. Sci. Lett. 71 (2), 229–240. https://doi.org/10.1016/0012-821X(84)90089-X.

Cerling, T.E., Quade, J., 1992. Isotopic evidence for climatic, ecologic, and faunal change in the Siwaliks of Pakistan. Paleontol.Soc.Specl Publ. 6, 54. https://doi.org/10.1017/S2475262200006146.
Cerling, T.E., Quade, J., Wang, Y., Bowman, J.R., 1989. Carbon isotopes in soils and palaeosols as ecology and palaeoecology indicators. Nature 341 (6238), 138–139. https://doi.org/10.1038/341138a0.
Chadwick, O.A., Gavenda, R.T., Kelly, E.F., Ziegler, K., Olson, C.G., Elliott, W.C., Hendricks, D.M., 2003. The impact of climate on the biogeochemical functioning of volcanic soils. Chem. Geol. 202 (3–4), 195–223. https://doi.org/10.1016/j.chemgeo.2002.09.001.
Deressa, A., Yli-Halla, M., Mohamed, M., Wogi, L., 2018. Soil classification of humid Western Ethiopia: a transect study along a toposequence in Didessa watershed. Catena 163, 184–195. https://doi.org/10.1016/j.catena.2017.12.020.
Dorji, T., Caspari, T., Bäumler, R., Veldkamp, A., Jongmans, A., Tshering, K., Baillie, I., 2009. Soil development on Late Quaternary river terraces in a high montane valley in Bhutan, Eastern Himalayas. Catena 78 (1), 48–59. https://doi.org/10.1016/j.catena.2009.02.018.
Driese, S.G., Nordt, L.C., Lynn, W.C., Stiles, C.A., Mora, C.I., Wilding, L.P., 2005. Distinguishing climate in the soil record using chemical trends in a Vertisol climosequence from the Texas coast prairie, and application to interpreting Paleozoic paleosols in the Appalachian Basin, USA. J. Sediment. Res. 75 (3), 339–349. https://doi.org/10.2110/jsr.2005.027.
Deutz, P., Montanez, I.P., Monger, H.C., Morrison, J., 2001. Morphology and isotope heterogeneity of Late Quaternary pedogenic carbonates: implications for paleosol carbonates as paleoenvironmental proxies. Palaeogeogr. Palaeoclimatol. Palaeoecol. 166 (3–4), 293–317.
Dorale, J.A., Edwards, R.L., Ito, E., González, L.A., 1998. Climate and vegetation history of the midcontinent from 75 to 25 ka: a speleothem record from Crevice Cave, Missouri, USA. Science 282 (5395), 1871–1874.
Eppes, M.C., Bierma, R., Vinson, D., Pazzaglia, F., 2008. A soil chronosequence study of the Reno valley, Italy: insights into the relative role of climate versus anthropogenic forcing on hillslope processes during the mid-Holocene. Geoderma 147 (3–4), 97–107. https://doi.org/10.1016/j.geoderma.2008.07.011.
Ehleringer, J.R., Cerling, T.E., Helliker, B.R., 1997. C4 photosynthesis, atmospheric CO2, and climate. Oecologia 112 (3), 285–299. https://doi.org/10.1007/s004420050311.
Fredlund, G.G., Tieszen, L.L., 1997. Phytolith and carbon isotope evidence for late Quaternary vegetation and climate change in the southern Black Hills,South Dakota. Quat. Res. 47 (2), 206–217. https://doi.org/10.1006/qres.1996.1862.
Gardner, L.R., Diffendal Jr., R., Williams, D.F., 1992. Stable isotope composition of calcareous paleosols and ground-water cements from the Ogallala Group (Neogene), western Nebraska. Contributions to Geology, University of Wyoming 29, 97–109.
Gee, G.W., Bauder, W., 1986. Principle of the pipette method. In: Agronomy: Methods of Soil Analysis.Part I: Physical and Mineralogical Methods. American Society of Agronomy, Madison, pp. 394–396.
Gocke, M., Pustovoytov, K., Kühn, P., Wiesenberg, G.L., Löscher, M., Kuzyakov, Y., 2011. Carbonate rhizoliths in loess and their implications for paleoenvironmental reconstruction revealed by isotopic composition: δ13C, 14C. Chem. Geol. 283 (3–4), 251–260. https://doi.org/10.1016/j.chemgeo.2011.01.022.
Humphrey, J.D., Ferring, C.R., 1994. Stable isotopic evidence for latest Pleistocene and Holocene climatic change in north-Central Texas. Quat. Res. 41 (2), 200–213. https://doi.org/10.1006/qres.1994.1022.
Jacobs, P.M., Mason, J.A., 2005. Impact of Holocene dust aggradation on a horizon characteristics and carbon storage in loess-derived Mollisols of the Great Plains, USA. Geoderma 125 (1–2), 95–106. https://doi.org/10.1016/j.geoderma.2004.07.002.
Jacobs, P.M., Mason, J.A., 2007. Late Quaternary climate change, loess sedimentation, and soil profile development in the central Great Plains: a pedosedimentary model. Geol. Soc. Am. Bull. 119 (3–4), 462–475. https://doi.org/10.1130/B25868.1.
Jenny, H., 1941. Factors of Soil Formation. Soil Sci. 52 (5), 415. https://doi.org/10.1097/00010694-194111000-00009.
Johnson, B.G., Layzell, A.L., Eppes, M.C., 2015. Chronosequence development and soil variability from a variety of sub-alpine, post-glacial landforms and deposits in the southeastern San Juan Mountains of Colorado. Catena 127, 222–239. https://doi.org/10.1016/j.catena.2014.12.026.
Johnson, W.C., Willey, K.L., 2000. Isotopic and rock magnetic expression of environmental change at the Pleistocene-Holocene transition in the central Great Plains. Quat. Int. 67 (1), 89–106. https://doi.org/10.1016/S1040-6182(00)00011-2.
Johnson, W.C., Willey, K.L., Mason, J.A., May, D.W., 2007. Stratigraphy and environmental reconstruction at the middle Wisconsinan Gilman Canyon formation type locality, Buzzard's Roost, southwestern Nebraska, USA. Quat. Res. 67, 474–486. https://doi.org/10.1016/j.yqres.2007.01.011[Opens in a new window].
Kelly, E.F., Amundson, R.G., Marino, B.D., DeNiro, M.J., 1991. Stable carbon isotopic composition of carbonate in Holocene grassland soils. Soil Sci. Soc. Am. J. 55 (6), 1651–1658. https://doi.org/10.2136/sssaj1991.03615995005500060025x.
Knapp, A.K., Chen, A., Griffin-Nolan, R.J., Baur, L.E., Carroll, C.J., Gray, J.E., Hoffman, A.M., Li, X., Post, A.K., Slette, I.J., Collins, S.L., Luo, Y., Smith, M.D., 2020. Resolving the Dust Bowl paradox of grassland responses to extreme drought. Proc. Natl. Acad. Sci. 117 (36), 22249–22255. https://doi.org/10.1073/pnas.1922030117.
Kohn, M.J., 2010. Carbon isotope compositions of terrestrial C3 plants as indicators of (paleo) ecology and (paleo) climate. Proc. Natl. Acad. Sci. U.S.A. 107 (46), 19691–19695. https://doi.org/10.1073/pnas.1004933107.
Kraimer, R.A., Monger, H.C., 2009. Carbon isotopic subsets of soil carbonate—a particle size comparison of limestone and igneous parent materials. Geoderma 150 (1–2), 1–9. https://doi.org/10.1016/j.geoderma.2008.11.042.
Layzell, A.L., Mandel, R.D., 2020. Late Quaternary landscape evolution and bioclimatic change in the central Great Plains, USA. Geol. Soc. Am. Bull. 132 (11–12), 2553–2571. https://doi.org/10.1130/B35462.1.
Layzell, A.L., Eppes, M.C., Lewis, R.Q., 2012. A soil chronosequence study on terraces of the Catawba River near Charlotte, NC: insights into the long-term history evolution of a major eastern seaboard Atlantic Piedmont drainage basin. Southeast. Geol. 49 (4).
Layzell, A.L., Mandel, R.D., Ludvigson, G.A., Rittenour, T.M., Smith, J.J., 2015. Forces driving late Pleistocene (ca. 77–12 ka) landscape evolution in the Cimarron River valley, southwestern Kansas. Quat. Res. 84 (1), 106–117. https://doi.org/10.1016/j.yqres.2015.05.003.
Layzell, A.L., Mandel, R.D., Rittenour, T.M., Smith, J.J., Harlow, R.H., Ludvigson, G.A., 2016. Stratigraphy, morphology, and geochemistry of late Quaternary buried soils on the High Plains of southwestern Kansas, USA. Catena 144, 45–55. https://doi.org/10.1016/j.catena.2016.05.003.
Mandel, R.D., 2008. Buried Paleoindian-age landscapes in stream valleys of the Central Plains, USA. Geomorphology 101 (1–2), 342–361. https://doi.org/10.1016/j.geomorph.2008.05.031.
Mandel, R.D., Bettis III, E.A., 1995. Late Quaternary landscape evolution and stratigraphy in Eastern Nebraska. In: Flowerday, C.A. (Ed.), Geologic Field Trips in Nebraska and Adjacent Parts of Kansas and South Dakota, vol. 10. Conservation and Survey Division, Institute of Agriculture and Natural Resources, University of Nebraska-Lincoln, Guidebook, pp. 77–90.
Mandel, R.D., Bettis, E.A., Hanson, P.R., 2016. Characteristics and geochronology of the Severance Formation: A new mid-through late Wisconsinan lithostratigraphic unit in the eastern plains of North America. Geological Society of America Abstracts with Programs 48 (7).
Mason, J.A., Jacobs, P.M., Hanson, P.R., Miao, X.D., Goble, R.J., 2003. Sources and paleoclimatic significance of Holocene Bignell Loess, central Great Plains, USA. Quat. Res. 60, 330–339. https://doi.org/10.1016/j.yqres.2003.07.005.
Mason, J.A., Joeckel, R.M., Bettis III, E.A., 2007. Middle to late Pleistocene loess record in eastern Nebraska, USA, and implications for the unique nature of Oxygen Isotope Stage 2. Quat. Sci. Rev. 26, 773–792. https://doi.org/10.1016/j.quascirev.2006.10.007.
Michel, L.A., Driese, S.G., Nordt, L.C., Breecker, D.O., Labotka, D.M., Dworkin, S.I., 2013. Stable-isotope geochemistry of vertisols formed on marine limestone and implications for deep-time paleoenvironmental reconstructions. J. Sediment. Res. 83 (4), 300–308. https://doi.org/10.2110/jsr.2013.26.
Michel, L.A., Tabor, N.J., Montañez, I.P., 2016. Paleosol diagenesis and its deep-time paleoenvironmental implications, Pennsylvanian-Permian Lodeve Basin,France. J. Sediment. Res. 86 (7), 813–829. https://doi.org/10.2110/jsr.2016.41.
Monger, H.C., Cole, D.R., Gish, J.W., Giordano, T.H., 1998. Stable carbon and oxygen isotopes in Quaternary soil carbonates as indicators of ecogeomorphic changes in the northern Chihuahuan Desert, USA. Geoderma 82 (1–3), 137–172. https://doi.org/10.1016/S0016-7061(97)00100-6.
Mintz, J.S., Driese, S.G., Breecker, D.O., Ludvigson, G.A., 2011. Influence of changing hydrology on pedogenic calcite precipitation in Vertisols, Dance Bayou, Brazoria County, Texas, USA: implications for estimating paleoatmospheric pCO2. J. Sediment. Res. 81 (6), 394–400. https://doi.org/10.2110/jsr.2011.36.
Montañez, I.P., 2013. Modern soil system constraints on reconstructing deep-time atmospheric CO2. Geochim. Cosmochim. Acta. 101, 57–75. https://doi.org/10.1016/j.gca.2012.10.012.
Muhs, D.R., Bettis, E.A., Aleinikoff, J.N., McGeehin, J.P., Beann, J., Skipp, G., Benton, R., 2008. Origin and paleoclimatic significance of late Quaternary loess in Nebraska: evidence from stratigraphy, chronology, sedimentology, and geochemistry. Geol. Soc. Am. Bull. 120, 1378–1407. https://doi.org/10.1130/B26221.1.
Mullin, M.R., 2010. Stable Isotope Record of Soil Carbonates from the Eocene-Oligocene Transition, Badlands National Park, South Dakota, USA. Ball State University, Muncie, Indiana. MS thesis.
Nordt, L., Von Fischer, J., Tieszen, L., Tubbs, J., 2008. Coherent changes in relative C4 plant productivity and climate during the late Quaternary in the North American Great Plains. Quat. Sci. Rev. 27 (15–16), 1600–1611. https://doi.org/10.1016/j.quascirev.2008.05.008.
Pendall, E.G., Harden, J.W., Trumbore, S.E., Chadwick, O.A., 1994. Isotopic approach to soil carbonate dynamics and implications for paleoclimatic interpretations. Quat. Res. 42 (1), 60–71. https://doi.org/10.1006/qres.1994.1054.
Quade, J., Cerling, T.E., Bowman, J.R., 1989. Development of Asian monsoon revealed by marked ecological shift during the latest Miocene in northern Pakistan. Nature 342 (6246), 163–166. https://doi.org/10.1038/342163a0.
Reed, E.C., Dreeszen, V.H., 1965. Revision of the classification of the pleistocene deposits of Nebraska. Nebraska Geol. Survey Bull. 23, 65 pp.
Schoeneberger, P.J., Wysocki, D.A., Benham, E.C., Broderson, W.D., 2012. Field Book for Describing and Sampling Soils: Lincoln, Nebraska, National Soil Survey Center, U.S. Department of Agriculture, v. 2.0, 228 p.
Souders, V.L., Kuzila, M.S., 1990. A report on the geology and radiocarbon ages of four superimposed horizons at a site in the Republican River valley, Franklin County Nebraska. Proceedings of the Nebraska Academy of Sciences, 65.
Stevenson, B.A., Kelly, E.F., McDonald, E.V., Busacca, A.J., 2005. The stable carbon isotope composition of soil organic carbon and pedogenic carbonates along a bioclimatic gradient in the Palouse region, Washington State, USA. Geoderma 124 (1–2), 37–47. https://doi.org/10.1016/j.geoderma.2004.03.006.
Stiles, C.A., Mora, C.I., Driese, S.G., Robinson, A.C., 2003. Distinguishing climate and time in the soil record: mass-balance trends in Vertisols from the Texas coastal prairie. Geology 31 (4), 331–334. https://doi.org/10.1130/0091-7613(2003)031<0331:DCATIT>2.0.CO;2.

Tecsa, V., Mason, J.A., Johnson, W.C., Miao, X., Constantin, D., Radu, S., Magdas, D.A., Veres, D., Markovic, S.B., Timar-Gabor, A., 2020. Latest Pleistocene to Holocene loess in the central Great Plains: Optically stimulated luminescence dating and multi-proxy analysis of the enders loess section (Nebraska, USA). Quat. Sci. Rev. 229, 106130 https://doi.org/10.1016/j.quascirev.2019.106130.

Terri, J.A., Stowe, L.G., 1976. Climatic patterns and the distribution of C4 grasses in North America. Oecologia 23, 1–12. https://doi.org/10.1007/BF00351210.

Tabor, N.J., Myers, T.S., Gulbranson, E., Rasmussen, C., Sheldon, N.D., Driese, S.G., Nordt, L.C., 2013. Carbon stable isotope composition of modern calcareous soil profiles in California: implications for CO2 reconstructions from calcareous paleosols. In: New Frontiers in Paleopedology and Terrestrial Paleoclimatology, Vol. 104. SEPM (Society for Sedimentary Geology)., pp. 17–34

Treadwell-Steitz, C., McFadden, L.D., 2000. Influence of parent material and grain size on carbonate coatings in gravelly soils, Palo Duro Wash, New Mexico. Geoderma 94 (1), 1–22. https://doi.org/10.1016/S0016-7061(99)00075-0.

Tonkin, P.J., Basher, L.R., 2001. Soil chronosequences in subalpine superhumid Cropp Basin, western Southern Alps, New Zealand. N. Z. J. Geol. Geophys. 44 (1), 37–45. https://doi.org/10.1080/00288306.2001.9514920.

Turner, B.L., Hayes, P.E., Laliberté, E., 2018. A climosequence of chronosequences in southwestern Australia. Eur. J. Soil Sci. 69 (1), 69–85. https://doi.org/10.1111/ejss.12507.

Voelker, A.H., 2002. Global distribution of centennial-scale records for Marine Isotope Stage (MIS) 3: a database. Quat. Sci. Rev. 21 (10), 1185–1212.

von Fischer, J.C., Tieszen, L.L., Schimel, D.S., 2008. Climate controls on C3 vs. C4 productivity in North American grasslands from carbon isotope composition of soil organic matter. Glob. Chang. Biol. 14 (5), 1141–1155. https://doi.org/10.1111/j.1365-2486.2008.01552.x.

Wang, Y., Cerling, T.E., Effland, W.R., 1993. Stable isotope ratios of soil carbonate and soil organic matter as indicators of forest invasion of prairie near Ames,Iowa. Oecologia 95 (3), 365–369. https://doi.org/10.1007/BF00320990.

Wang, Y., McDonald, E., Amundson, R., McFadden, L., Chadwick, O., 1996. An isotopic study of soils in chronological sequences of alluvial deposits, Providence Mountains, California. Geol.Soc.Am.Bull. 108 (4), 379–391. https://doi.org/10.1130/0016-7606(1996)108<0379:AISOSI>2.3.CO;2.

Webb, T.H., Campbell, A.S., Fox, F.B., 1986. Effect of rainfall on pedogenesis in a climosequence of soils near Lake Pukaki, New Zealand. N. Z. J. Geol. Geophys. 29 (3), 323–334. https://doi.org/10.1080/00288306.1986.10422155.

Wynn, J.G., 2007. Carbon isotope fractionation during decomposition of organic matter in soils and paleosols: implications for paleoecological interpretations of paleosols. Palaeogeogr. Palaeoclimatol. Palaeoecol. 251 (3–4), 437–448. https://doi.org/10.1016/j.palaeo.2007.04.009.

Yair, A., 1990. The role of topography and surface cover upon soil formation along hillslopes in arid climates. Geomorphology 3 (3–4), 287–299. https://doi.org/10.1016/0169-555X(90)90008-E.

Yang, Y., Mason, J.A., Zhang, H., Lu, H., Ji, J., Chen, J., Liu, L., 2017. Provenance of loess in the central Great Plains, USA based on Nd-Sr isotopic composition, and paleoenvironmental implications. Quat. Sci. Rev. 173, 114–123. https://doi.org/10.1016/j.quascirev.2017.08.009.